Exercise reverses preamyloid oligomer and prolongs survival in αB-crystallin-based desmin-related cardiomyopathy

Alina Maloyan*, James Gulick*, Charles G. Glabe†, Rakez Kayed†, and Jeffrey Robbins*‡

*Department of Pediatrics, Cincinnati Children's Hospital Medical Center, Cincinnati, OH 45229; and †Department of Molecular Biology and Biochemistry, University of California, Irvine, CA 92697

Edited by Eric N. Olson, University of Texas Southwestern Medical Center, Dallas, TX, and approved February 20, 2007 (received for review October 18, 2006)

The R120G mutation in the small heat shock-like protein αB-crystallin (CryAB^{R120G}) causes desmin-related myopathy (DRM), which is characterized by the formation of desmin- and CryAB-containing aggregates within muscle fibers. Mice with cardiac-specific overexpression of CryAB^{R120G} develop cardiomyopathy at 3 months and die at 6–7 months from heart failure (HF). Previous studies showed that overexpression of CryAB^{R120G} results in accumulation of preamyloid oligomer (PAO). PAO is considered to be the cytotoxic entity in many of the protein misfolding-based neurodegenerative diseases. On the basis of data from mouse models of neurodegenerative diseases showing that exercise or environmental enrichment reduces the amyloid oligomer level and improves cognitive ability, we hypothesized that CryAB^{R120G}-induced DRM would also respond favorably to prolonged voluntary exercise, reducing HF symptoms and rescuing the mice from premature death. Six months of voluntary exercise in CryAB^{R120G} animals resulted in 100% survival at a time when all unexercised mice had died. After 22 weeks of exercise, PAO levels were decreased by 47% compared with the unexercised CryAB^{R120G} control mice ($P = 0.00001$). Although CryAB^{R120G} expression led to decreased levels of the metallomembrane endopeptidase neprilysin, normal levels were maintained in the exercised CryAB^{R120G} mice, and *in vitro* loss-of-function and gain-of-function experiments using adenovirus-infected cardiomyocytes confirmed the importance of neprilysin in ameliorating PAO accumulation. The data demonstrate that voluntary exercise slows the progression to HF in the CryAB^{R120G} DRM model and that PAO accumulation is mediated, at least in part, by decreased neprilysin activity.

cardiac | disease | heart | transgenic

Desmin-related myopathy (DRM) belongs to the family of protein-misfolding diseases and is associated with mutations in desmin, αB-crystallin (CryAB) (1), and selenoproteins (1, 2). Multiple mutations in CryAB can cause human DRM, and one of the mutations, resulting in a change from arginine to glycine at residue 120 (CryAB^{R120G}), has been modeled in transgenic (TG) mice (3). Cardiomyocyte-specific overexpression of CryAB^{R120G} resulted in dilated cardiomyopathy by 3 months, with the animals developing heart failure (HF) and dying by 6–7 months (4). CryAB-DRM is characterized by the accumulation of desmin- and CryAB-containing aggresomes, which are large perinuclear protein depositions formed by microtubule-dependent accumulation of small aggregates that initially develop at the cell periphery (5). Aggresomes are associated with the protein conformation-based neurodegenerative disorders (5–8). Accumulation of misfolded or unfolded proteins underlies the pathogenesis of most amyloid-based neurodegenerative diseases such as Alzheimer's disease and Parkinson's disease, in which aggregates containing the mutant protein develop via reorganization of soluble monomers into prefibrillar oligomers. These can coalesce into protofilaments, which then go on to form the characteristic amyloid-positive tangles and/or plaques (9). Recent data show a poor correlation between the mature plaques and disease severity (10), and, for at least some of the neurodegenerative disorders, it is the soluble, preamyloid oligomers (PAOs) that are the most potent mediators of cytotoxicity (11). Data in support of this hypothesis have also been gathered by using animal models in which the development of structural and functional neuronal deficits substantially preceded the formation of amyloid plaques (12).

Recent data have uncovered several parallels between CryAB^{R120G}-induced DRM and the neurodegenerative diseases. First, as is the case for a number of the neurodegenerative diseases, CryAB^{R120G}-DRM is associated with cytoplasmic accumulation of misfolded proteins within inclusion bodies (13). Second, an antibody that recognizes the toxic conformer shared between PAOs that form from diverse, amyloidogenic proteins (14) reacts strongly to material present in neurons derived from various neurodegenerative diseases as well as from CryAB^{R120G}-positive cardiomyocytes (13, 15). For both the neurodegenerative and CryAB^{R120G}-based cardiac diseases, disease severity correlates directly with levels of the antibody-reactive, PAO material rather than with aggresomes or amyloid-positive plaques or tangles, and the data are consistent with the contribution of PAO to CryAB^{R120G}-induced pathogenesis (15). Third, like neurodegenerative diseases, CryAB^{R120G}-DRM progression strongly correlates with mitochondrial dysfunction, particularly with inhibition of complex I (16).

Results obtained from mouse models of neurodegenerative disease show that environmental enrichment or voluntary exercise is beneficial in terms of delayed onset and progression of disease (17–20). Investigators modeled human physical, social, and intellectual enrichment by placing at least two animals in large cages with running wheels, toys, and colorful tunnels (21). A physical component of environmental enrichment has particular clinical importance. Voluntary exercise delayed the onset of neurological deficits in a mouse model of Huntington's disease (20), and long-term exercise decreased the amyloid load in a mouse model of Alzheimer's disease (19). Voluntary exercise of mice housed in cages with running wheels resulted in significant decreases in neural amyloid deposits and enhanced learning ability compared with nonexercised littermates (17). On the basis of these data and the parallels between the neurodegenerative disorders and CryAB^{R120G}-induced cardiomyopathy, we

Author contributions: A.M. and J.R. designed research; A.M. performed research; J.G., C.G.G., and R.K. contributed new reagents/analytic tools; A.M. and J.R. analyzed data; and A.M. and J.R. wrote the paper.

The authors declare no conflict of interest.

This article is a PNAS Direct Submission.

Abbreviations: DRM, desmin-related myopathy; TG, transgenic; NTG, nontransgenic; NTGtr, NTG exercised; TGtr, TG exercised; PAO, preamyloid oligomer; CryAB, αB-crystallin; NRC, neonatal rat cardiomyocyte; HF, heart failure.

‡To whom correspondence should be addressed at: Cincinnati Children's Hospital Medical Center, MLC 7020, 3333 Burnet Avenue, Cincinnati, OH 45229. E-mail: jeff.robbins@cchmc.org.

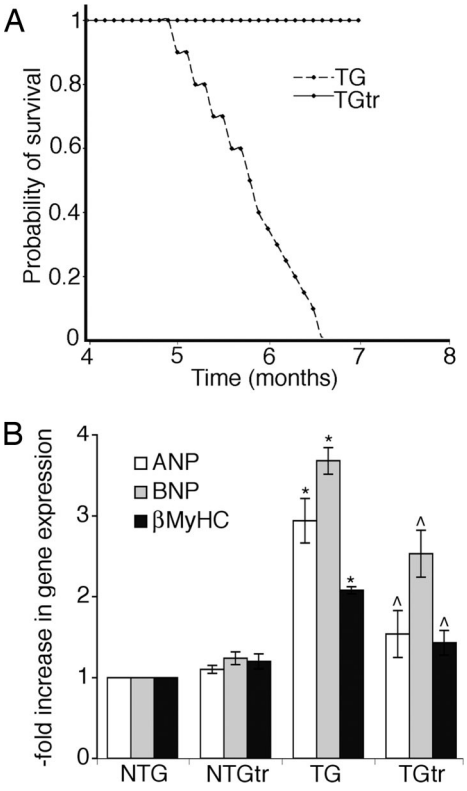

Fig. 1. Voluntary exercise. (*A*) Kaplan–Meier curves for exercised (solid line) and unexercised (broken line) CryAB^{R120G} mice. (*B*) Quantitative PCR analysis revealed that voluntary exercise significantly attenuated activation of the fetal gene program that is normally observed in the CryAB^{R120G} TG mice. *, significant difference vs. NTG ($P < 0.05$); ∧, significant difference vs. unexercised TG ($P < 0.05$).

tested the effects of long-term voluntary exercise in the CryAB^{R120G}-DRM model. The data show that exercise led to significant reductions of PAO with a concomitant increase in lifespan.

Results

To investigate the effects of exercise on CryAB^{R120G}-induced HF, 24 1-month-old males from nontransgenic (NTG) and TG groups were housed in regular cages (control groups) or in cages equipped with voluntary running wheels (exercised groups) with two mice per cage. All CryAB^{R120G} TG mice from the unexercised group died from HF by 6 months (Fig. 1*A*). Despite developing heart disease in the TG cohorts, there were no significant differences between the TG and NTG cohorts in distances run in the early and mid-phases of the study (data not shown). Our analyses subsequently focused on the exercised and unexercised CryAB^{R120G} TG groups. After 22 weeks of exercise the mice underwent echocardiographic assessment, which showed modest differences in the heart rates between the two groups but no significant differences in functional parameters (Table 1). Running did produce the expected reduction in body weight in both groups. Strikingly, voluntary running appeared to be cardioprotective, with all members of the exercised group alive after all CryAB^{R120G} mice housed in the cages without the wheels had died (Fig. 1*A*).

Hypertrophied and failing hearts are often characterized by activation of the fetal gene program (4). Consistent with the developing cardiac pathology, at 28 weeks in the unexercised TG animals, atrial natriuretic peptide, β-myosin heavy chain, and brain natriuretic peptide, which are all characteristic of murine cardiac fetal gene expression and/or adult cardiac hypertrophy, were significantly elevated. The hearts isolated from the exercised TG cohorts showed a significant attenuation of this response (Fig. 1*B*).

CryAB^{R120G}-mediated DRM belongs to the family of protein-misfolding diseases and is characterized by the formation of CryAB- and desmin-containing aggregates as well as high concentrations of PAO in the cardiomyocytes (13). In previous studies the viability of CryAB^{R120G} TG mice was linked to decreased PAO deposition but was independent of aggregate concentrations (15). To determine the effect of voluntary exercise on the accumulation of aggregates and PAO, we probed heart sections with anti-CryAB and anti-PAO antibodies (Fig. 2). Accumulations of the CryAB-positive aggregates were identical between the exercised and unexercised TG groups after 22 weeks of exercise (Fig. 2 *A* and *B*). We then probed the sections with anti-PAO antibody (14) after 1 month, 3 months, and 6 months of exercise and observed progressive reductions in PAO deposition in the hearts of exercised compared with unexercised TG mice (Fig. 2 *C* and *D*). Morphometric analysis revealed a 47% decrease of PAO immunoreactivity in the exercised animals compared with the control group at 6 months (Fig. 2*D*).

Progression of HF is often associated with cardiomyocyte apoptosis (22). Our previous study revealed significant activation of apoptosis in the CryAB^{R120G} hearts (16). Given the above data that exercise reduces PAO accumulation and prolongs life, we tested the hypothesis that exercise decreased activation of apoptosis in the CryAB^{R120G}-induced HF model. A critical step in the development of apoptotic cell death is caspase-3 cleavage and the subsequent cleavage of its substrates. Low levels of cleaved caspase-3 were detected in NTG and exercising TG mice (Fig. 3*A*). In contrast, the control TG group showed dramatic increases in the level of cleaved protein, and, as early as 2 months, cleavage of two of its substrates, Rho-associated coiled-coil protein kinase and poly-(ADP-ribose)-polymerase, was apparent in the unexercised but not in the exercised mice. At termination (6 months), we quantitated the number of TUNEL-positive cardiomyocytes as a marker for DNA fragmentation and

Table 1. Echocardiography of mouse groups

Mouse group	Body weight, g	Heart weight, g	Heart rate, beats/min	IVS		SF, %
				Diastole	Systole	
NTG	32.92 ± 0.7	0.236 ± 0.02	432.22 ± 24.9	0.09 ± 0.01	0.13 ± 0.01	41.22 ± 1.1
NTGtr	31.03 ± 0.06*	0.219 ± 0.01	468.4 ± 23.01	0.09 ± 0.01	0.13 ± 0.01	44.16 ± 2.4
TG	33.26 ± 0.7	0.38 ± 0.03*	306.2 ± 9.8*	0.14 ± 0.01*	0.18 ± 0.01*	31.7 ± 1.5*
TGtr	30.73 ± 1.07*†	0.36 ± 0.03*	388.92 ± 24.9†	0.14 ± 0.02*	0.17 ± 0.01*	30.3 ± 3.1*

NTGtr and TGtr mice were allowed access to cage wheel exercise. Shown are average values ± SE for 7-month-old TGtr mice and 6-month-old TG mice ($n = 6$ for each group). IVS, intraventricular septum; SF, shortening fraction. *, significant difference vs. NTG ($P < 0.001$); †, significant difference vs. unexercised TG ($P < 0.001$).

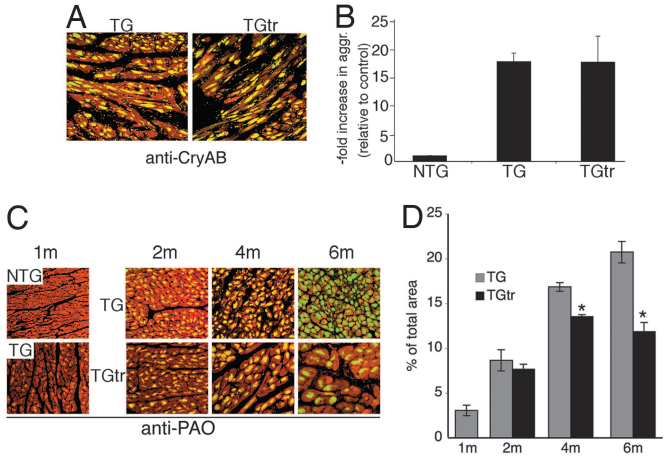

Fig. 2. Long-term voluntary exercise and aggregate accumulation. Mice were aged for 1 month and then divided into the exercised and unexercised groups. (*A*) Cardiomyocytes were identified by phalloidin (red fluorescence). Anti-CryAB (green fluorescence) staining in the unexercised CryAB^{R120G} (TG) and exercised CryAB^{R120G} hearts was used to detect aggresome accumulation. The mice were exercised for 22 weeks. (*B*) Aggresomes were quantitated by using the filtration assay. (*C*) PAO levels were determined before the exercise regimen when the mice were 1 month old. PAO levels were then determined after 1 month, 3 months, and 6 months of exercise (2m, 4m, and 6m, respectively). Cardiomyocytes were identified by phalloidin (red fluorescence). PAO was detected by using the A11 antibody (green fluorescence) in the unexercised CryAB^{R120G} (TG) and exercised CryAB^{R120G} hearts. (*D*) Quantitative analysis of the amount of A11 immunoreactivity, expressed as a percentage of total area of each section ± SE. *, significant difference vs. unexercised TG ($P <$ 0.005).

found that exercise training decreased DNA fragmentation by 70% compared with the control TG group (Fig. 3*B*).

Because PAO accumulation is directly correlated with the severity of cardiac disease (15), we examined the potential causes for its accumulation. Recent data indicate that amyloid-rich neural samples from patients with neurodegenerative disease show significantly reduced levels of the metallomembrane endopeptidase neprilysin (23–25). The formation of amyloid and preamyloid depositions can be enzymatically regulated by this enzyme (23), and we hypothesized that PAO accumulation in the hearts of CryAB^{R120G} mice might be partially dependent on diminished neprilysin activity. Neprilysin mRNA and protein levels in the hearts from NTG animals (data not shown), as well

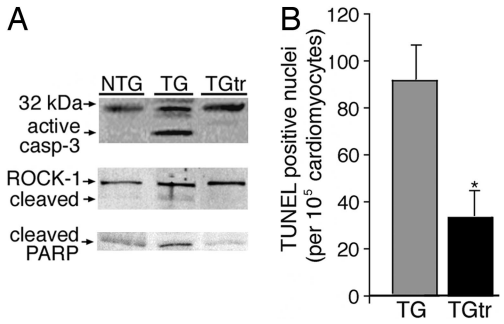

Fig. 3. The effect of long-term voluntary exercise on apoptotic cell death in CryAB^{R120G} mice. Mice were housed for 6 months. (*A*) Caspase-3 activation in the nonexercised and exercised mice was determined, as was the cleaved forms of two of its substrates, Rho-associated coiled-coil protein kinase 1 (ROCK-1) and poly-(ADP-ribose)-polymerase (PARP) (46), early in the trial at 2 months. (*B*) Quantitation of TUNEL-stained nuclei in frozen sections from exercised and unexercised CryAB^{R120G} hearts. *, significant difference vs. unexercised TG ($P <$ 0.005).

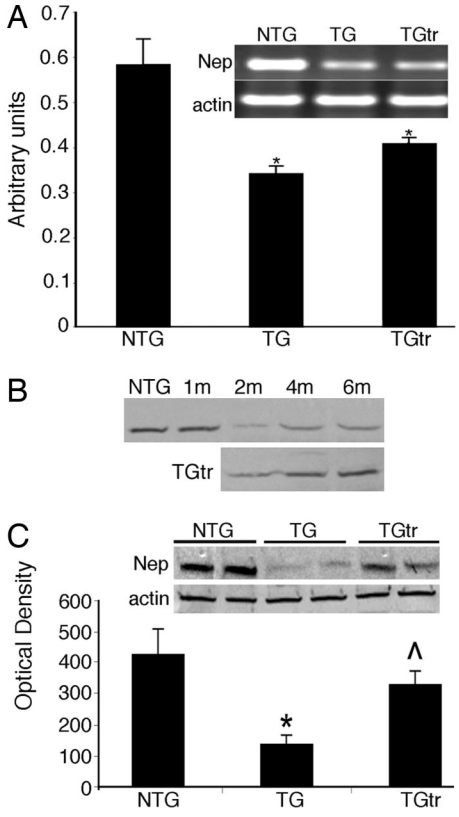

Fig. 4. CryAB^{R120G} expression decreases neprilysin levels. (*A*) Semiquantitative RT-PCR analysis of neprilysin mRNA. All data points were taken from cycle 24, which was in the linear range of the reaction. Neprilysin RNA was significantly reduced in both the unexercised and exercised hearts. (*B*) Time course of neprilysin protein reduction. Shown are the Western blots prepared from the same groups used to derive the data shown in Fig. 2*C*. The mice were allowed access to the wheels starting at 1 month (1m). (*C*) Exercise conserves normal neprilysin protein levels. The representative Western blot data and quantitation show significant conservation of normal neprilysin levels in the exercised CryAB^{R120G} hearts. β-Actin was used as a loading control. Volume is expressed in arbitrary units ± SE. *, significant difference vs. NTG ($P < 0.001$); ∧, significant difference vs. unexercised TG ($P < 0.001$); $n = 6$.

as the exercised and unexercised TG mice, were determined (Fig. 4). At the end of the 6-month trial, whereas neprilysin levels were not affected by exercise in the NTG animals, we observed significant reductions in both neprilysin mRNA and protein in the unexercised CryAB^{R120G} mice relative to NTG and exercised CryAB^{R120G} hearts (Fig. 4). The time course of reduced neprilysin protein reduction (Fig. 4*B*) closely matched the time course observed for PAO accumulation (Fig. 2*C*). In the exercised CryAB^{R120G} hearts, although RNA levels remained low, quantitation of neprilysin protein confirmed nearly normal levels.

To better understand the inverse correlation between neprilysin levels and PAO accumulation we used neonatal rat cardiomyocyte (NRC) cultures. Adenovirus-mediated CryAB^{R120G} expression in NRCs leads to PAO accumulation within 72–96 h (13). NRC transfected with adenovirus carrying CryAB^{R120G} showed decreased neprilysin levels after only 24 h of culture (Fig. 5*A*). To test the hypothesis that inhibition of neprilysin activity accelerates PAO accumulation, we cultured the nontransfected and transfected cells with and without the addition of thiorphan, an inhibitor of neprilysin enzymatic activity. Thiorphan treatment had no effect on neprilysin levels (Fig. 5*A*) but led to precocious accumulation of PAO-positive material within 24 h of infection (Fig. 5*B*). Elevated PAO levels due to increased NO production as a result of thiorphan treatment were ruled out by

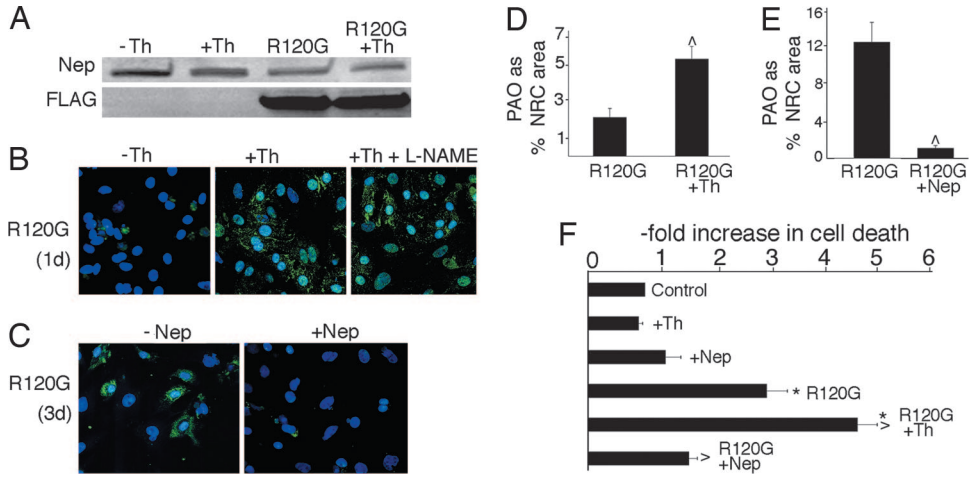

Fig. 5. Neprilysin plays a causative role in PAO accumulation. (*A*) Representative Western blot showing neprilysin levels in untreated NRCs and CryAB^{R120G}-infected NRCs in the presence or absence of thiorphan 24 h after infection. (*B*) PAO accumulation (green) in CryAB^{R120G}-infected NRCs 24 h after infection was enhanced by thiorphan. Nuclei (blue) were stained with TO-PRO-3. To confirm that the increased PAO levels were not due to NO production, the NO synthase inhibitor N^G-nitro-L-arginine methyl ester (L-NAME) was also added to selected cultures. (*C*) Overexpression of neprilysin significantly reduces PAO 3 days after infection. (*D* and *E*) Quantitation of PAO-positive areas from *B* and *C*, respectively, as a percentage of total NRC area. (*F*) The effect of overexpression or inhibition of neprilysin on the rate of cardiac cell death as measured by the release of adenylate kinase into the medium. Values shown are the average-fold increase relative to control, nontransfected NRCs for three independent series ± SE. *, $P < 0.005$ vs. control; ∧, $P < 0.005$ vs. CryAB^{R120G}-infected NRCs.

the addition of the NO synthase inhibitor N^G-nitro-L-arginine methyl ester to selected cultures (Fig. 5*B*). To further study the role of neprilysin in the formation of PAO, we prepared an adenovirus expressing mouse neprilysin. Adenovirus carrying the construct resulted in an ≈10-fold increase in neprilysin levels relative to unaffected cardiomyocytes (data not shown) and partially abolished PAO accumulation 3 days after infection (Fig. 5*C*). Quantitation confirmed a >2-fold increase ($P < 0.005$) in PAO as a result of neprilysin inhibition (Fig. 5*D*). Conversely, overexpression of neprilysin led to a 12-fold reduction in PAO relative to the NRCs infected with CryAB^{R120G} alone (Fig. 5 *C* and *E*). Consistent with PAO's toxic effects, cotransfection of adeno-CryAB^{R120G} with the neprilysin adenovirus construct led to significantly reduced cell death compared with those transfected with CryAB^{R120G} alone (Fig. 5*F*).

Discussion

Cardiac pathology develops over a period of 5–7 months in the mouse model of CryAB^{R120G}-DRM, resulting in HF and death. Although many factors, such as mitochondrial dysfunction and disruption of the contractile apparatus, are involved during progression of the disease (1, 4, 16, 26), our recent studies showed a strong correlation between PAO levels and cardiac dysfunction (13, 15). Formation of prefibrillar oligomeric deposits from amyloidogenic proteins is now thought to be a primary cytotoxic event in the protein conformation, amyloidogenic diseases (11, 12). However, it should be emphasized that CryAB^{R120G}-DRM does not appear to be a classic amyloidosis, which is characterized by the accumulation of amyloid plaques or insoluble fibrils. Amyloids are classically defined by Congo red or thioflavin T staining and green birefringence under polarized light, and appear as unbranched, 10-nm fibrils in the electron microscope (27). Although CryAB^{R120G} aggregates do stain with Congo red, we have not observed the characteristic "apple green" birefringence, and electron microscopy studies failed to detect the characteristic amyloid fibrils in CryAB^{R120G} TG hearts (unpublished data).

Using inducible cardiomyocyte-based TG CryAB^{R120G} expression, we showed that cessation of CryAB^{R120G} synthesis 2–3 weeks before death rescued the TG mice and was accompanied by significant reductions in PAO levels (15). We hypothesized that environmental enrichment, which was effective in reducing brain amyloid levels in mouse models suffering from neurodegenerative disease (17–19), might impact favorably on PAO formation and delay or even halt the cascade of pathological events leading to HF. The results strikingly paralleled those obtained with the inducible system, in that voluntary exercise resulted in a 47% decrease in PAO levels, and this was accompanied by 100% survival rather than 100% mortality. Thus, two disparate approaches yielded the same result, the commonality being decreased PAO levels directly correlating with improved survival.

Unlike our more intense, forced exercise models (28), the relatively mild nature of the voluntary exercise is underscored by the lack of any increase in cardiac mass in the exercised animals. In fact, voluntary exercise actually had a potentially beneficial effect on the hypertrophy program, reducing reactivation of fetal gene expression, which often precedes and accompanies pathological hypertrophy (29). Exercise also had a beneficial effect on the apoptotic index in the CryAB^{R120G} hearts (16) with both TUNEL-positive nuclei and activated caspase-3 levels reduced. These results are in agreement with previous studies indicating the antiapoptotic effect of exercise training (30–32). Although voluntary exercise had no effect on the functional parameters measured by echocardiography, these data are consistent with a clinical trial in which 100 chronic HF patients were enlisted. Although moderate long-term exercise did result in improvements in both quality of life and cardiac function, the parameters determined by echocardiography showed no differences between the exercised and nonexercised groups (33). It is unclear what the outcome of more intensive, forced exercise regimens such as swimming or running on a motorized, incline treadmill would be. Under certain conditions, exercise is clearly beneficial, and, in a hypertrophic cardiomyopathic mouse model carrying a mutation in the gene that encodes the predominant cardiac myosin heavy chain, voluntary cage wheel running prevented onset of cardiac pathology and ameliorated existing pathology when initiated in older animals (30). However, intense exercise is associated with sudden cardiac death in symptomatic and asymptomatic heart disease resulting from different etiologies (34), and, for humane reasons, we have not subjected obviously ill mice to high-stress exercise. We hypothesize that one would observe, as cardiac function decreased, an increased inci-

dence in sudden death that would overshadow any potential decrease in PAO.

Neprilysin, also known as neutral endopeptidase (EC3.4.24.11), is a zinc metallopeptidase that is widely distributed in the body and actively degrades a variety of peptides in the immune, circulatory, and nervous systems (35–37). A genetic deficiency in neprilysin results in accumulation of amyloid-β in the brain (23). TG or viral expression of neprilysin in the brains of amyloid-β precursor protein (APP) TG mice led to marked improvement in amyloid-β pathology (38, 39). Exposure of APP TG mice to an enriched environment resulted in attenuation in cerebral amyloid-β levels and amyloid deposits, with a concomitant elevation of brain neprilysin activity (19). Additionally, neprilysin was found to be reduced in the areas of the brain that are vulnerable for amyloid plaque formation (40), and a causative role of reduced neprilysin activity in the development of the memory-associated symptoms of Alzheimer's disease has been proposed (41). In the heart, neprilysin contributes significantly to the degradation of the vasodilator and antifibrotic peptide bradykinin and to the degradation of the vasodilator and antihypertrophic peptides ANP and brain natriuretic protein (35). Upregulation of myocardial neprilysin mRNA, protein expression, and enzymatic activity has been described in the failing human heart (42), and neprilysin inhibition effectively increases bradykinin-mediated vasodilatation as well as net tissue plasminogen activator release (43). In contrast with those data, failing CryAB^{R120G} TG hearts showed significantly decreased neprilysin levels, and this appears to be true in other genetically induced murine HF models as well (A.M. and J.R., unpublished results). However, restoration of normal neprilysin levels in the exercised TG group correlated directly to decreased PAO levels, a result consistent with the data obtained in the Alzheimer's disease models noted above (38, 44). Our data show that, in cardiomyocyte cultures, CryAB^{R120G} expression reduced neprilysin levels within a matter of days and that specific inhibition of neprilysin activity by thiorphan results in significant acceleration of PAO accumulation and increased cytotoxicity. Finally, adenovirus-mediated expression of neprilysin in CryAB^{R120G}-transfected NRCs inhibited PAO accumulation. It is unclear whether the inhibitory effect is due to decreased formation of PAO deposits, acceleration of their degradation, or a combination of the two, and detailed *in vitro* studies using recombinant proteins will be needed to distinguish between these processes. In any case, our data do introduce a cautionary note for the use of neprilysin inhibitors in heart disease because such treatment may lead to increased PAO levels, placing an unexpected pathogenic burden on an already compromised heart.

In previous studies we showed abundant amounts of intracellular PAO deposits in patients with HF from diverse causes (13). It would be of interest to determine whether exercise can have an impact on human cardiac PAO levels as well. However, inhibition of neprilysin activity for 14–30 days may delay progression of human HF (42), and it will be important to determine in the mouse models whether modulation of neprilysin activity during the progression of cardiac disease has long-term therapeutic effects.

Materials and Methods

TG Mice. Male FVB/N mice with cardiac-specific overexpression of a mutated CryAB containing the R120G missense mutation (CryAB^{R120G}) have been described (4).

NRC Cultures and Adenovirus Infection. NRCs were isolated under standard conditions and grown in 10-cm plates or in two-well chambered glass slides coated with gelatin. Replication-deficient recombinant adenoviruses were prepared by using the AdEasy system (Stratagene, La Jolla, CA). CryAB^{R120G} adenovirus was prepared as described previously (13). The mouse neprilysin clone was purchased from Invitrogen (Carlsbad, CA) (ID no. 4483558, GenBank accession no. BC034092) and used as a template for RT-PCR. The PCR product was ligated into a Topo blunt vector (Invitrogen), sequenced, and then cloned into the SalI–HindIII-digested pShuttle-CMV vector (Clontech, Mountain View, CA). A multiplicity of infection of 10 was used for both viruses to infect the cardiomyocyte cultures. Cellular toxicity was measured by adenylate kinase release into the medium 4 days after transfection by using the Toxilight assay (Cambrex, North Brunswick, NJ).

Immunohistochemistry. Immunohistochemical analyses were performed as described before (13, 15). Anti-CryAB was purchased from Stressgen (San Diego, CA) (SPA-223), anti-neprilysin was from R & D Systems (Minneapolis, MN), and anti-oligomer A11 antibody has been described (14). Anti-FLAG antibody was from Stratagene. Alexa Fluor 488-conjugated anti-rabbit, phalloidin-Alexa Fluor 568, and To-Pro-3 for nuclear staining were purchased from Invitrogen. The intensity of PAO staining was quantified by using MetaMorph (version 7; Molecular Devices, Sunnyvale, CA). The averaged area of PAO staining was normalized to total cardiomyocyte area. The aggregates were quantified by using a filter retention assay as described, with the precipitated aggregate captured on the nitrocellulose membrane and quantitated by incubation with anti-CryAB antibody (45).

RT-PCR. RNA extraction using TRIREAGENT (Molecular Research Center, Cincinnati, OH) was carried out according to the manufacturer's protocol. RT-PCR was performed with the SuperScript III First Strand Synthesis system (Invitrogen) by using primers as follows. Neprilysin, 5′-GTGCTCGGCAGTCCAACTCATTGAAC-3′ (sense) and 5′-GGAAGACTTCCTGTTTCTGTGGCTTTG-3′ (antisense); β-actin, 5′-CTTCGCGGGCGACGATGCTC-3′ (sense) and 5′-CTACGTACATGGCTGGGGTGTTGAAG-3′ (antisense). Denaturation was carried out at 94°C for 35 sec, followed by 45 sec of annealing at 55°C and 1 min of extension at 72°C. Quantitative real-time PCR used a PTC-200 DNA Engine cycler (Bio-Rad, Hercules, CA) and the TaqMan gene expression assays (Applied Biosystems, Foster City, CA) and was performed by using the manufacturer's protocol with the prevalidated primers and TaqMan probes for the individual target RNAs. Each RNA was quantified in duplicate and normalized to the level of GAPDH.

This work was supported by National Institutes of Health Research Grants R01 HL69799, HL60546, HL52318, HL60546, and HL56370 (to J.R.) and by the American Heart Association, Great Rivers Affiliate (A.M.).

1. Goldfarb LG, Vicart P, Goebel HH, Dalakas MC (2004) *Brain* 127:723–734.
2. Ferreiro A, Ceuterick-de Groote C, Marks JJ, Goemans N, Schreiber G, Hanefeld F, Fardeau M, Martin JJ, Goebel HH, Richard P, *et al.* (2004) *Ann Neurol* 55:676–686.
3. Vicart P, Caron A, Guicheney P, Li Z, Prevost MC, Faure A, Chateau D, Chapon F, Tome F, Dupret JM, *et al.* (1998) *Nat Genet* 20:92–95.
4. Wang X, Osinska H, Klevitsky R, Gerdes AM, Nieman M, Lorenz J, Hewett T, Robbins J (2001) *Circ Res* 89:84–91.
5. Kopito RR (2000) *Trends Cell Biol* 10:524–530.
6. Johnston JA, Ward CL, Kopito RR (1998) *J Cell Biol* 143:1883–1898.
7. Junn E, Lee SS, Suhr UT, Mouradian MM (2002) *J Biol Chem* 277:47870–47877.
8. Buckig A, Tikkanen R, Herzog V, Schmitz A (2002) *Histochem Cell Biol* 118:353–360.
9. Soto C (2003) *Nat Rev Neurosci* 4:49–60.
10. Zerovnik E (2002) *Eur J Biochem* 269:3362–3371.
11. Meredith SC (2006) *Ann NY Acad Sci* 1066:181–221.
12. Hsia AY, Masliah E, McConlogue L, Yu GQ, Tatsuno G, Hu K, Kholodenko D, Malenka RC, Nicoll RA, Mucke L (1999) *Proc Natl Acad Sci USA* 96:3228–3233.
13. Sanbe A, Osinska H, Saffitz JE, Glabe CG, Kayed R, Maloyan A, Robbins J (2004) *Proc Natl Acad Sci USA* 101:10132–10136.
14. Kayed R, Head E, Thompson JL, McIntire TM, Milton SC, Cotman CW, Glabe CG (2003) *Science* 300:486–489.

15. Sanbe A, Osinska H, Villa C, Gulick J, Klevitsky R, Glabe CG, Kayed R, Robbins J (2005) *Proc Natl Acad Sci USA* 102:13592–13597.
16. Maloyan A, Sanbe A, Osinska H, Westfall M, Robinson D, Imahashi K, Murphy E, Robbins J (2005) *Circulation* 112:3451–3461.
17. Adlard PA, Perreau VM, Pop V, Cotman CW (2005) *J Neurosci* 25:4217–4221.
18. Jankowsky JL, Melnikova T, Fadale DJ, Xu GM, Slunt HH, Gonzales V, Younkin LH, Younkin SG, Borchelt DR, Savonenko AV (2005) *J Neurosci* 25:5217–5224.
19. Lazarov O, Robinson J, Tang YP, Hairston IS, Korade-Mirnics Z, Lee VM, Hersh LB, Sapolsky RM, Mirnics K, Sisodia SS (2005) *Cell* 120:701–713.
20. van Dellen A, Blakemore C, Deacon R, York D, Hannan AJ (2000) *Nature* 404:721–722.
21. van Praag H, Kempermann G, Gage FH (2000) *Nat Rev Neurosci* 1:191–198.
22. Wencker D, Chandra M, Nguyen K, Miao W, Garantziotis S, Factor SM, Shirani J, Armstrong RC, Kitsis RN (2003) *J Clin Invest* 111:1497–1504.
23. Iwata N, Tsubuki S, Takaki Y, Shirotani K, Lu B, Gerard NP, Gerard C, Hama E, Lee HJ, Saido TC (2001) *Science* 292:1550–1552.
24. Carson JA, Turner AJ (2002) *J Neurochem* 81:1–8.
25. Carter TL, Pedrini S, Ghiso J, Ehrlich ME, Gandy S (2006) *Neurosci Lett* 392:235–239.
26. Wang X, Klevitsky R, Huang W, Glasford J, Li F, Robbins J (2003) *Circ Res* 93:998–1005.
27. Westermark P, Benson MD, Buxbaum JN, Cohen AS, Frangione B, Ikeda S, Masters CL, Merlini G, Saraiva MJ, Sipe JD (2005) *Amyloid* 12:1–4.
28. Fewell JG, Osinska H, Klevitsky R, Ng W, Sfyris G, Bahrehmand F, Robbins J (1997) *Am J Physiol* 273:H1595–H1605.
29. Vikstrom KL, Bohlmeyer T, Factor SM, Leinwand LA (1998) *Circ Res* 82:773–778.
30. Konhilas JP, Watson PA, Maass A, Boucek DM, Horn T, Stauffer BL, Luckey SW, Rosenberg P, Leinwand LA (2006) *Circ Res* 98:540–548.
31. Kwak HB, Song W, Lawler JM (2006) *FASEB J* 20:791–793.
32. Siu PM, Bryner RW, Martyn JK, Alway SE (2004) *FASEB J* 18:1150–1152.
33. Belardinelli R, Georgiou D, Cianci G, Purcaro A (1999) *Circulation* 99:1173–1182.
34. Maron BJ (2003) *N Engl J Med* 349:1064–1075.
35. Rademaker MT, Richards AM (2005) *Clin Sci (London)* 108:23–36.
36. Turner AJ, Brown CD, Carson JA, Barnes K (2000) *Adv Exp Med Biol* 477:229–240.
37. Turner AJ, Isaac RE, Coates D (2001) *BioEssays* 23:261–269.
38. Iwata N, Mizukami H, Shirotani K, Takaki Y, Muramatsu S, Lu B, Gerard NP, Gerard C, Ozawa K, Saido TC (2004) *J Neurosci* 24:991–998.
39. Leissring MA, Farris W, Chang AY, Walsh DM, Wu X, Sun X, Frosch MP, Selkoe DJ (2003) *Neuron* 40:1087–1093.
40. Reilly CE (2001) *J Neurol* 248:159–160.
41. Huang SM, Mouri A, Kokubo H, Nakajima R, Suemoto T, Higuchi M, Staufenbiel M, Noda Y, Yamaguchi H, Nabeshima T, *et al.* (2006) *J Biol Chem* 281:17941–17951.
42. Fielitz J, Dendorfer A, Pregla R, Ehler E, Zurbrugg HR, Bartunek J, Hetzer R, Regitz-Zagrosek V (2002) *Circulation* 105:286–289.
43. Cruden NL, Fox KA, Ludlam CA, Johnston NR, Newby DE (2004) *Hypertension* 44:913–918.
44. Shirotani K, Tsubuki S, Iwata N, Takaki Y, Harigaya W, Maruyama K, Kiryu-Seo S, Kiyama H, Iwata H, Tomita T, *et al.* (2001) *J Biol Chem* 276:21895–21901.
45. Wanker EE, Scherzinger E, Heiser V, Sittler A, Eickhoff H, Lehrach H (1999) *Methods Enzymol* 309:375–386.
46. Chang J, Xie M, Shah VR, Schneider MD, Entman ML, Wei L, Schwartz RJ (2006) *Proc Natl Acad Sci USA* 103:14495–14500.